

# A traffic flow lattice model considering relative current influence and its numerical simulation\*

Sun Di-Hua(孙隽华)<sup>a)</sup>, Tian Chuan(田川)<sup>a)†</sup>, and Liu Wei-Ning(刘卫宁)<sup>b)</sup>

<sup>a)</sup>College of Automation, Chongqing University, Chongqing 400030, China

<sup>b)</sup>College of Computer, Chongqing University, Chongqing 400030, China

(Received 11 December 2009; revised manuscript received 6 January 2010)

Based on Xue's lattice model, an extended lattice model is proposed by considering the relative current information about next-nearest-neighbour sites ahead. The linear stability condition of the presented model is obtained by employing the linear stability theory. The density wave is investigated analytically with the perturbation method. The results show that the occurrence of traffic jamming transitions can be described by the kink-antikink solution of the modified Korteweg-de Vries (mKdV) equation. The simulation results are in good agreement with the analytical results, showing that the stability of traffic flow can be enhanced when the relative current of next-nearest-neighbour sites ahead is considered.

**Keywords:** traffic flow, relative current, lattice model, numerical simulation

**PACC:** 0550, 0520

## 1. Introduction

Traffic problems, especially the traffic jam, has been a serious problem in modern society, and has attracted much attention in the past decades. To investigate the properties of traffic jams, many traffic models<sup>[1-17]</sup> are presented, among them, the most popular ones are the car following models, the cellular automaton models, the gas kinetic models, and the hydrodynamic models.

When vehicle density is high in a freeway, traffic jams occur and propagate as density waves. In the past, traffic jams have been investigated by making use of nonlinear analysis method. Based on hydrodynamic model, Korteweg-de Vries (KdV) equation was presented by Kurtze and Hong.<sup>[18]</sup> Their results showed that the traffic soliton can be observed near the neutral stability line. Modified KdV (mKdV) equation, which was derived from the optimal velocity model by Komatsu and Sasa,<sup>[19]</sup> illustrated that traffic jam could be described in terms of a kink density wave near the critical point. On the other hand, the mKdV equation from the hydrodynamic model was presented by Nagatani<sup>[20]</sup> and the density wave in congestion was thus described by this equation.

As one of the macroscopic traffic models, in 1998, Nagatani<sup>[20]</sup> proposed a simplified version of the hy-

drodynamic models which is convenient for analysing the density wave of traffic flow. A continuum model is adopted in this model to describe the jamming transition in traffic flow on highway, which is referred to as model I in Ref. [20] and is described as

$$\partial_t \rho + \rho_0 \partial_x (\rho v) = 0, \quad (1)$$

$$\partial_t \rho v = a \rho_0 V(\rho(x + \delta)) - a \rho v, \quad (2)$$

where  $\rho_0$  denotes the average density;  $a$  is the sensitivity of a driver;  $\rho(x + \delta)$  is the local density at position  $x + \delta$  and time  $t$ ;  $\delta$  represents the average headway, which means  $\delta = 1/\rho_0$ ; local density is expressed as  $\rho(x + \delta) = 1/h(x, t)$ , where  $h(x, t)$  is the headway. The right-hand side of Eq. (2) expresses the tendency of traffic flow  $\rho v$  at a given density to relax to some natural average flow  $\rho_0 V(\rho(x + \delta))$ .

The continuity equation (2) is modified with dimensionless space  $x$ . Let  $\tilde{x} = x/\delta$ , and  $\tilde{x}$  is indicated as  $x$  hereafter.

$$\partial_t \rho_j + \rho_0 (\rho_j v_j - \rho_{j-1} v_{j-1}) = 0, \quad (3)$$

$$\partial_t (\rho_j v_j) = a \rho_0 V(\rho_{j+1}) - a \rho_j v_j, \quad (4)$$

where  $j$  indicates the  $j$ -th site on a one-dimensional lattice;  $\rho_j(t)$  denotes the local density on site  $j$  at time  $t$ , and  $v_j(t)$  represents its corresponding local velocity, and  $V$  refers to the optimal velocity function.

\*Project supported by the National High Technology Research and Development Program of China (Grant No. 511-0910-1031).

†Corresponding author. E-mail: tianchuan\_168@163.com

After that, Xue<sup>[21]</sup> improved the lattice version of traffic model by considering the next-nearest-neighbour headway and described it as

$$\rho_j(t + \tau)v_j(t + \tau) = \rho_0 V(\rho_{j+1}(t))(1 - p) + \rho_0 V(\rho_{j+2}(t))p, \quad (5)$$

where  $p$  is a constant ranging 0–0.5 which means the front term plays a dominant role.

When economic value is concerned, it is of great significance to maximize the throughput of cars and suppress the traffic jam on highways.<sup>[22]</sup> However, these models mainly pay much attention to the effects of density and velocity of the sites. Here, we concentrate on the enhancement and the stabilization of traffic flow with other related information about the interaction on a single lane. In particular, the information about the relative current of two sites ahead may have an important effect on traffic flow. By introducing the relative current of two sites ahead, not only the stability of traffic flow can be improved, but also the appearance of traffic jams can be suppressed effectively.

Based on Xue's lattice model, an extended lattice version of the continuum model was presented in this paper by considering the relative current of the next-nearest-neighbour sites ahead, and then, linear stability theory and nonlinear analysis are applied to the extended model to derive the modified KdV equation near the critical point by the perturbation method. We analyse the effects of relative current of the next-nearest-neighbour sites on traffic stability and jam transition, and verified that the new consideration can effectively suppress the traffic jams by simulation.

The remainder of the present paper is organized as follows. In Section 2, we put forward the extended lattice model considering the density and the relative current of two sites ahead on a single-lane highway. In Section 3, we consider the effect of the relative current of the next-nearest-neighbour sites on the stability of traffic flow by using the linear stability theory, and the results show that the stability of traffic flow is enhanced apparently. In Section 4, by means of the nonlinear analysis, we derive the mKdV equation near the critical point and obtain its kink–antikink soliton solution to describe traffic jams. In Section 5, the model is simulated under the periodic boundary condition, and its result is in good agreement with the analytic one. In Section 6 we draw some conclusions from the present study.

## 2. Models

According to the idea mentioned above, and starting from Xue's model, we present an improved lattice model in which relative current effect of two front lattice sites is considered. The vehicle motion is described by the following differential–difference equations:

$$\partial_t \rho_j + \rho_0(\rho_j v_j - \rho_{j-1} v_{j-1}) = 0, \quad (6)$$

$$\rho_j(t + \tau)v_j(t + \tau) = \rho_0 V(\rho_{j+1}(t), \rho_{j+2}(t)) + kG(\Delta Q_j, \Delta Q_{j+1}), \quad (7)$$

where  $V(\rho_{j+1}, \rho_{j+2}) = (1 - p)V(\rho_{j+1}) + pV(\rho_{j+2})$ ,  $G(\Delta Q_j, \Delta Q_{j+1}) = (1 - p)\Delta Q_j + p\Delta Q_{j+1}$ ,  $\Delta Q_j = \rho_{j+1}v_{j+1} - \rho_j v_j$  and  $\Delta Q_{j+1} = \rho_{j+2}v_{j+2} - \rho_{j+1}v_{j+1}$  is the relative currents,  $p$  is a constant ranging 0–0.5 which means the front term plays a dominant role. Compared with Xue's model, our model has an interaction term that is different from that of Xue's model, in which the relative current is assumed not to contribute to the flux interaction. However, it is supposed in our model that the relative current of two sites ahead does influence the nature of traffic by response factor  $k$ . When  $k = 0$ , equations (6) and (7) of the extended model reduce into those of Xue's model. Equation (6) is the lattice version of a continuity equation, while equation (7) is the evolution equation,  $V(\rho)$  expresses the optimal velocity function and it decreases monotonically with upper bound. We adopt the same optimal velocity function as that used by Bando *et al.*<sup>[23]</sup> except for density variable

$$V(\rho) = \frac{V_{\max}}{2} \tanh\left(\frac{1}{\rho} - h_c\right) + \tanh(h_c), \quad (8)$$

where  $h_c = 4$  is the safety distance and  $V_{\max} = 2$  denotes the maximal velocity.

By eliminating the speed  $v$  in Eqs. (6) and (7), the density equations are obtained as follows:

$$\begin{aligned} \partial_t \rho_j(t + \tau) + \rho_0^2 & [(1 - p)(V(\rho_{j+1}) - V(\rho_j)) \\ & + p(V(\rho_{j+2}) - V(\rho_{j+1}))] \\ & - k[(1 - p)(\partial_t \rho_{j+1} - \partial_t \rho_j) \\ & + p(\partial_t \rho_{j+2} - \partial_t \rho_{j+1})] = 0. \end{aligned} \quad (9)$$

## 3. Linear stability analysis

We apply the linear stability method to the extended model to investigate the influence of the difference in relative current between two sites ahead on

traffic flow. First, we define the state of uniform traffic flow with constant density  $\rho_0$  and optimal velocity  $V(\rho_0)$ . The solution of the homogeneous traffic flow is given as

$$\rho_j(t) = \rho_0, \quad v_j(t) = V(\rho_0). \quad (10)$$

Assume that  $y_j(t)$  is a small deviation from the steady state flow:

$$\rho_j(t) = \rho_0 + y_j(t), \quad (11)$$

substituting Eq. (11) into Eq. (9) and linearize them, then we will obtain

$$\begin{aligned} \partial_t y_j(t + \tau) + \rho_0^2 V'(\rho_0) [(1-p)(y_{j+1}(t) - y_j(t)) \\ + p(y_{j+2}(t) - y_{j+1}(t))] \\ - k[(1-p)(\partial_t y_{j+1}(t) - \partial_t y_j(t)) \\ + p(\partial_t y_{j+2}(t) - \partial_t y_{j+1}(t))] = 0, \end{aligned} \quad (12)$$

where  $V'(\rho_0) = dV(\rho)d\rho|_{\rho=\rho_0}$ .

By expanding  $y_j(t) = \exp(ikj + zt)$ , we have the following equation of  $z$ :

$$\begin{aligned} ze^{zt} + \rho_0^2 V'(\rho_0) [(e^{ik} - 1)(1-p) + e^{ik}(e^{ik} - 1)p] \\ - kz [(e^{ik} - 1)(1-p) + e^{ik}(e^{ik} - 1)p] = 0. \end{aligned} \quad (13)$$

Inserting  $z = z_1 ik + z_2 (ik)^2 + \dots$  into Eq. (13) and neglecting the higher order terms yield the first order and second order terms as follows:

$$z_1 = -\rho_0^2 V'(\rho_0), \quad (14)$$

$$z_2 = -\left[ \frac{1+2p}{2} + \rho_0^2 V'(\rho_0)\tau + k \right] \rho_0^2 V'(\rho_0). \quad (15)$$

If  $z_2$  is a negative value, the uniformly steady-state flow becomes unstable for long-wavelength method, while the uniform flow is stable when  $z_2$  is a positive value, thus the neutral stable condition for this steady state is given by

$$\tau = -\left( \frac{1+2p}{2} + k \right) \frac{1}{\rho_0^2 V'(\rho_0)}. \quad (16)$$

For a small disturbance with long wavelength, the homogeneous traffic flow is stable on condition that

$$\tau < -\left( \frac{1+2p}{2} + k \right) \frac{1}{\rho_0^2 V'(\rho_0)}. \quad (17)$$

In comparison with Xue's model,<sup>[21]</sup> our extended model has a stable area that is enlarged obviously in the range

$$-\left( \frac{1+2p}{2} + k \right) \frac{1}{\rho_0^2 V'(\rho_0)} < \tau < -\frac{1+2p}{2(\rho_0^2 V'(\rho_0))},$$

which means that the traffic stability could be enhanced further by introducing the effect of relatively current of two lattice sites ahead.

The neutral stability lines in the parameter space  $(\rho, a)$  is shown in Fig. 1 by the solid lines for the extended model.

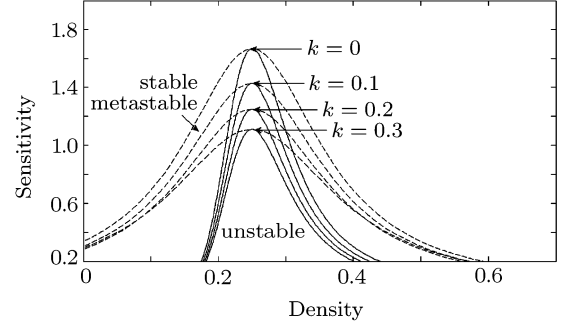


Fig. 1. Phase diagram in parameter space  $(\rho, a)$ .

In Fig. 1, the dot lines represent the coexisting curves obtained from the solution of the mKdV equation (see Section 4). There exists the critical point  $(\rho_c, a_c)$  which is the apex of the neutral stability line. In Fig. 1, the traffic flow is divided into three regions: the region above the coexisting curve, which represents the stability region; the metastable region lying between the neutral stability line and the coexisting curve; the region below the neutral stability line, is the unstable region. Traffic flow is stable above the neutral stability line where traffic jam will not appear, however, under the neutral stability line, traffic flow is unstable and the density waves occur. Furthermore, in Fig. 1, we can find out that with the value of  $k$  increasing, the critical points and the neutral stability line lower accordingly, which means that the traffic flow is stabilized further when the relative current of two sites ahead is considered. When  $k = 0$ , the neutral stability line is the same as that of Xue's model.

## 4. Nonlinear analysis and mKdV equation

In this section, the reductive perturbation method is applied to Eq. (9) and the system behaviour near the critical point  $(\rho_c, a_c)$  is deeply analysed. With such a simplification, the nature of kink-antikink solitons can be described by the mKdV equation.

We introduce slow scales for space variable  $j$  and time variable  $t$ , and define slow variable  $X$  and  $T$  as follows:<sup>[19,24]</sup>

$$X = \varepsilon(j + bt) \quad \text{and} \quad T = \varepsilon^3 t, \quad 0 < \varepsilon \leq 1, \quad (18)$$

where  $b$  is a constant to be determined. Letting

$$\rho_j(t) = \rho_c + \varepsilon R(X, T), \quad (19)$$

substituting Eqs. (18) and (19) into Eq. (9) and making the Taylor expansion to the fifth order of  $\varepsilon$  lead to the following expression:

$$\begin{aligned} &\varepsilon^2(b + \rho_c^2 V') \partial_X R + \varepsilon^3 \left( b^2 \tau + \frac{\rho_c^2 V'}{2} + \rho_c^2 V' p - kb \right) \partial_X^2 R \\ &+ \varepsilon^4 \left[ \partial_T R + \left( \frac{b^3 \tau^2}{2} + \frac{\rho_c^2 V'}{6} + p \rho_c^2 V' - \frac{1+2p}{2} bk \right) \partial_X^3 R + \frac{\rho_c^2 V'''}{6} \partial_X R^3 \right] \\ &+ \varepsilon^5 \left[ (2b\tau - k) \partial_T \partial_X R + \left( \frac{b^4 \tau^3}{6} + \frac{1+14p}{24} \rho_c^2 V' - \frac{6p+1}{6} bk \right) \partial_X^4 R + \frac{1+2p}{12} \rho_c^2 V'' \partial_X^2 R^3 \right] = 0, \end{aligned} \quad (20)$$

where  $V' = [dV(\rho_j)/d\rho_j]|_{\rho_j=\rho_c}$ , and  $V''' = [d^3V(\rho_j)/d\rho_j^3]|_{\rho_j=\rho_c}$ , with  $V'$  and  $V'''$  corresponding to  $V'(\rho_c)$  and  $V'''(\rho_c)$  in the above equation and hereafter. Near the critical point  $(\rho_c, a_c)$ ,  $\tau = (1 + \varepsilon^2)\tau_c$ , taking  $b = -\rho_c^2 V'$  and eliminating the second order and third order terms of  $\varepsilon$  from Eq. (20) result in the simplified equation:

$$\varepsilon^4 [\partial_T R - g_1 \partial_X^3 R + g_2 \partial_X R^3] + \varepsilon^5 [g_3 \partial_X^2 R + g_4 \partial_X^4 R + g_5 \partial_X^2 R^3] = 0, \quad (21)$$

where

$$\begin{aligned} g_1 &= \frac{3(\rho_c^2 V' \tau_c)^2 - 1 - 6p - 3k - 6pk}{6} \rho_c^2 V', \quad g_2 = \frac{\rho_c^2 V'''}{6}, \quad g_3 = (\rho_c^2 V')^2 \tau_c, \\ g_4 &= \left[ \frac{1 + 14p - 4(2b\tau_c - k)(1 + 6p)}{24} - \frac{3kb^2 \tau_c^2 - 5b^3 \tau_c^3 + 3k(2b\tau_c - k)(1 + 2p) - k(6p + 1)}{6} \right] \rho_c^2 V', \end{aligned}$$

and  $g_5 = \frac{1 + 2p - 4b\tau_c + 2k}{12} \rho_c^2 V'''$ .

In order to derive the regularized equation, we make the following transformations for Eq. (21):

$$T' = g_1 T, \quad R = \sqrt{\frac{g_1}{g_2}} R'. \quad (22)$$

We have the standard mKdV equation with an  $O(\varepsilon)$  correction term as follows:

$$\partial_{T'} R' - \partial_X^3 R' + \partial_X R'^3 + \varepsilon M[R'] = 0, \quad (23)$$

where

$$M[R'] = \frac{1}{g_1} \left[ g_3 \partial_X^2 R' + g_4 \partial_X^4 R' + \frac{g_1 g_5}{g_2} \partial_X^2 R'^3 \right]. \quad (24)$$

Ignore the  $O(\varepsilon)$  term, then we will obtain the mKdV equation with the kink-antikink soliton solution

$$R'_0(X, T') = \sqrt{c} \tanh \sqrt{\frac{c}{2}} (X - cT'). \quad (25)$$

With the method described in Ref. [25], we obtain the selected velocity  $c$

$$c = \frac{5g_2 g_3}{2g_2 g_4 - 3g_1 g_5}. \quad (26)$$

Hence, we obtain the kink-antikink soliton solution as follows:

$$\rho_j(t) = \rho_c + \sqrt{\frac{g_1 c}{g_2} \left( \frac{\tau}{\tau_c} - 1 \right)} \tanh \sqrt{\frac{c}{2} \left( \frac{\tau}{\tau_c} - 1 \right)}$$

$$\times \left[ j + \left( 1 - c g_1 \left( \frac{\tau}{\tau_c} - 1 \right) \right) t \right]. \quad (27)$$

Then, amplitude  $A$  of the kink-antikink soliton is given by

$$A = \sqrt{\frac{g_1 c}{g_2} \left( \frac{\tau}{\tau_c} - 1 \right)}. \quad (28)$$

The kink-antikink soliton represents coexisting phases, which consist of the freely moving phase at low density and the jammed phase at high density. The densities corresponding to the freely moving phase and the jammed phase are given, respectively, by  $\rho_j = \rho_c + A$  and  $\rho_j = \rho_c - A$ . Thus we can obtain the coexisting curve in the  $(\rho, a)$  parameter space (see Fig. 1).

## 5. Numerical simulation

For the convenience of simulation, we rewrite Eq. (9) into difference form

$$\begin{aligned} &\rho_j(t + 2\tau) - \rho_j(t + \tau) + \tau \rho_0^2 [(1-p)(V(\rho_{j+1}) \\ &- V(\rho_j)) + p(V(\rho_{j+2}) - V(\rho_{j+1}))] \\ &- k[(1-p)(\Delta \rho_j(t + \tau) - \Delta \rho_j(t)) \\ &+ p(\Delta \rho_{j+1}(t + \tau) - \Delta \rho_{j+1}(t))] = 0, \end{aligned} \quad (29)$$

where  $\Delta\rho_j = \rho_{j+1} - \rho_j$ , using the method mentioned in Section 2 yields the stability condition as follows:

$$\tau < -\frac{1 + 2p + 2k}{3\rho_0^2 V'(\rho_0)}. \quad (30)$$

The extended model described by Eq. (29) is simulated by using the periodic boundary condition. The initial conditions are chosen as follows:  $\rho_j(0) =$

$\rho_0 = 0.25, \rho_j(1) = \rho_j(0) = 0.25$ , for  $j \neq 50, 51$ ,  $\rho_j(1) = 0.25 - 0.1$  for  $j = 50$ , and  $\rho_j(1) = 0.25 + 0.1$  for  $j = 51$ , where the total number of sites is  $N = 100$ , the safety density is  $\rho_c = 0.25$ , and the sensitivity  $a = 1.67$ .

The typical traffic patterns can be observed in Fig. 2 after a sufficient long time (at least  $t = 10^4$ ).

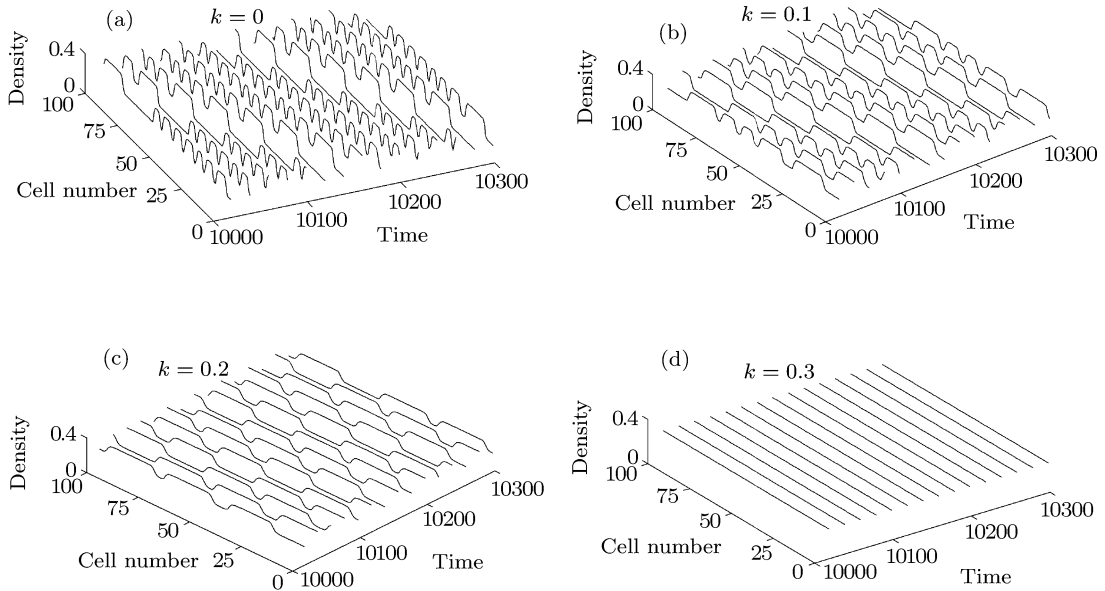


Fig. 2. Spatiotemporal evolutions of density for (a)  $k = 0$ , (b)  $k = 0.1$ , (c)  $k = 0.2$  and (d)  $k = 0.3$  ( $a = 1.67$ ,  $p = 0.1$ ).

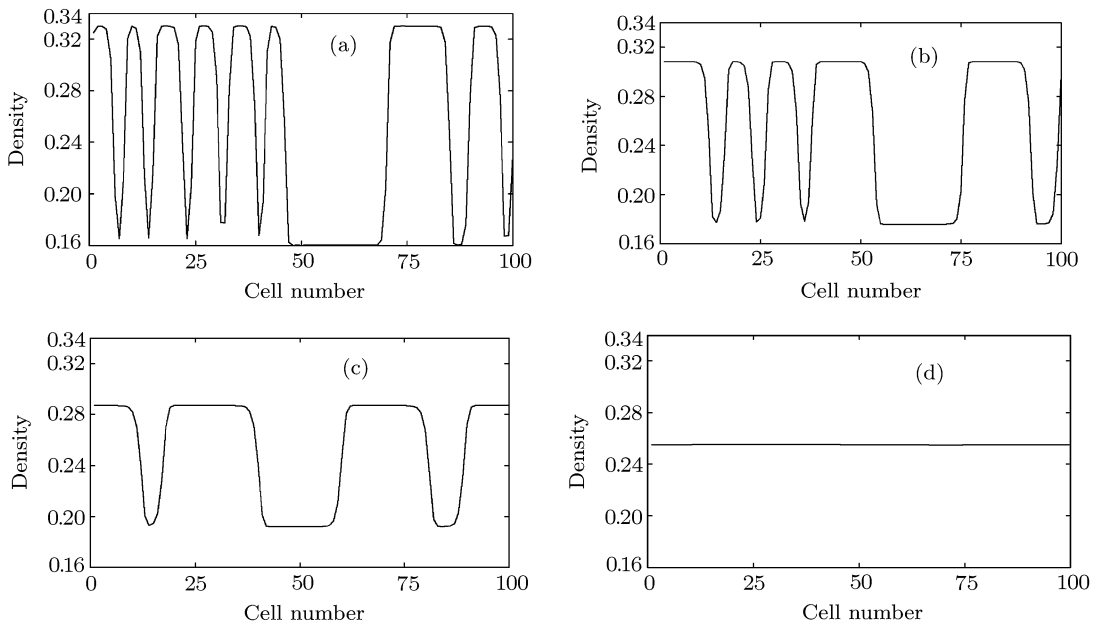


Fig. 3. Density profiles of the density wave at  $t = 10200$  correspond to the panels in Fig. 2 respectively.

Figure 2 shows that for various values of  $k$ , the spatiotemporal evolution of the density exhibit different properties correspondingly. When  $p = 0.1$ , the time evolutions of the density profile according to the extended model for  $k = 0, 0.1, 0.2$ , and  $0.3$  are shown in patterns (a), (b), (c) and (d) respectively. Pattern (a) with  $k = 0$  corresponds to that of the Xue's model. In patterns (a), (b) and (c), the traffic flows are unstable because stability condition (30) is not satisfied. When a small disturbance is added to the uniform traffic flow, the traffic flow transits from free flow to congested traffic, and the propagating backward kink-antikink density wave appears. However, under the same sensitivity, the pattern (d) exhibits the freely moving phase, which demonstrates that the relative current of two sites ahead should be considered.

Figure 3 shows the density profiles obtained at  $t = 10200$  corresponding to the panels in Fig. 2 respectively.

With the same sensitivity, when the value of sensitivity coefficient  $k$  increases, the amplitude of density wave weakens and the initial small disturbance delays.

If we set  $k = 0.3$ , density wave disappears and traffic flow turns uniform over the whole space in pattern (d).

Consequently, we can conclude from all the results that considering the effect of the relative current of two sites ahead can stabilize the traffic flow further and suppress traffic jams efficiently.

## 6. Conclusion

By introducing the relative current of two sites ahead into the Xue's model, an extended lattice model is presented in this paper to suppress traffic jams. We worked out the stability criterion of the proposed model through the linear stability analysis, and showed that the stability of traffic flow is enhanced by introducing the new consideration. Moreover, the kink-antikink soliton solution of the mKdV equation near the critical point is derived and used to describe the traffic jam by nonlinear analysis method. The good agreement between numerical simulation results and linearly analytical results verifies that our consideration is reasonable.

## References

- [1] Peng G H, Sun D H and He H P 2008 *Acta Phys. Sin.* **57** 7541 (in Chinese)
- [2] Xue Y, Dong L Y, Yuan Y W and Dai S Q 2002 *Acta Phys. Sin.* **51** 492 (in Chinese)
- [3] Mo Y L, He H D, Xue Y, Shi W and Lu W Z 2008 *Chin. Phys. B* **17** 4446
- [4] Chen X, Gao Z Y, Zhao X M and Jia B 2007 *Acta Phys. Sin.* **56** 2024 (in Chinese)
- [5] Li X L, Kuang H, Song T, Dai S Q and Li Z P 2008 *Chin. Phys. B* **17** 2366
- [6] Ge H X, Zhu H B and Dai S Q 2005 *Acta Phys. Sin.* **54** 4621 (in Chinese)
- [7] Tang T Q, Huang H J, Wong S C and Jiang R 2009 *Chin. Phys. B* **18** 975
- [8] Peng G H, Sun D H and He H P 2009 *Chin. Phys. B* **18** 468
- [9] Ge H X, Dai S Q and Dong L Y 2008 *Chin. Phys. B* **17** 23
- [10] Sun D H and Peng G H 2009 *Chin. Phys. B* **18** 3724
- [11] Treiber M, Hennecke A and Helbing D 1999 *Phys. Rev. E* **59** 239
- [12] Tian J F, Jia B, Li X G and Gao Z Y 2010 *Chin. Phys. B* **19** 010511
- [13] Sheng P, Zhao S L, Wang J F, Tang P and Gao L 2009 *Chin. Phys. B* **18** 3347
- [14] Peng G H and Sun D H 2009 *Chin. Phys. B* **18** 5420
- [15] Peng L J and Kang R 2009 *Acta Phys. Sin.* **58** 830 (in Chinese)
- [16] Kang R, Peng L J and Yang K 2009 *Acta Phys. Sin.* **58** 451 (in Chinese)
- [17] Zhao S G 2009 *Acta Phys. Sin.* **58** 7497 (in Chinese)
- [18] Kurtze D A and Hong D C 1995 *Phys. Rev. E* **52** 218
- [19] Komatsu T and Sasa S 1995 *Phys. Rev. E* **52** 5574
- [20] Nagayani T 1998 *Physica A* **261** 599
- [21] Xue Y 2004 *Acta Phys. Sin.* **53** 25 (in Chinese)
- [22] Helbing D and Huberman B A 1998 *Nature* **396** 738
- [23] Bando M, Hasebe K, Nakayama A, Shibata A and Sugiyama Y 1995 *Phys. Rev. E* **51** 1035
- [24] Nagitani T and Nakanishi K 1998 *Physica A* **31** 5431
- [25] Ge H X, Cheng R J and Dai S Q 2005 *Physica A* **357** 466